Physicochemical Evaluation and Insights into the Biological Efficacy of Vandetanib-Eluting Radiopaque Beads

Alice Hagan[1,2], Sami Znati[3], Rebecca Carter[3], Adam Westhorpe[3], Wendy M MacFarlane[2], Gary Phillips[2], Andrew W Lloyd[2], Ricky A Sharma[3] Andrew Lewis[1]

1) *Biocompatibles UK Ltd, a BTG International group company, Lakeview, Riverside Way, Watchmoor Park, Camberley, GU15 3YL, UK*

2) *School of Pharmacy and Biomolecular Sciences, University of Brighton, Moulsecoomb, Brighton BN2 4GJ, UK*

3) *NIHR University College London Hospitals Biomedical Research Centre, UCL Cancer Institute, Paul O'Gorman Building, 72 Huntley Street, London, WC1E 6AG, UK*

Abstract

Vandetanib-eluting radiopaque beads (VERB) have been developed for use in transarterial chemoembolisation of liver tumours. However, it is not known how embolisation-induced hypoxia may affect anti-tumoural activity of vandetanib. We studied the physicochemical properties of VERB, the efficacy of vandetanib against HCC cells in hypoxic conditions, as well as the direct effects of beads on 3D HCC spheroids. Vandetanib suppressed proliferation and induced apoptosis in HCC cells and endothelial cells *in vitro*, without signs of hypoxia-induced drug resistance. High degrees of apoptosis were observed among cells in which vandetanib suppressed ERK1/2 and upregulated the proapoptotic protein Bim, but this did not appear essential for vandetanib-induced cell death in all cell lines. Vandetanib also suppressed the expression of VEGF and it induced autophagy, including data suggestive of a cytoprotective role for the latter. Incubation of tumour spheroids with VERB led to sustained growth inhibition equivalent to the effect of free drug. We conclude that vandetanib and VERB are effective at inhibiting growth of HCC cells in hypoxic conditions, warranting their further evaluation as novel anticancer agents.

Introduction

Trans-arterial chemo-embolisation (TACE) is a minimally invasive treatment for liver tumours that combines local delivery of chemotherapy drugs with physical occlusion of tumour-feeding blood vessels, in order to induce necrosis by oxygen and nutrient deprivation. Drug-eluting embolisation beads (DEB) simultaneously reduce tumour blood perfusion and deliver high, sustained and precise intra-tumoural doses of therapeutic agents [1], beneficial for maintaining durable pharmacological activity . This creates an opportunity for delivery of drugs that require higher concentrations to be effective, for example doxorubicin. We have previously shown that the multi-targeted tyrosine kinase inhibitor vandetanib can be loaded on to DEBs [2], a drug delivery approach that reduces systemic exposure and therefore toxicity for the patient.

DEB delivery could also favour the use of drugs that show superior efficacy in hypoxic conditions induced by embolization of arteries, a characteristic which has not been demonstrated with the most

commonly used TACE drugs, e.g. anthracyclines [3]. Hypoxia is known to induce chemo-resistance in cancer cells [4]. Ischaemic conditions generated by the embolic effect of TACE may involuntarily promote survival of the remaining viable tumour by inducing hypoxia inducible factor (HIF)-mediated survival pathways such as metastasis, increased proliferation and drug resistance. In studies conducted in both animal models and human HCC patients, increased HIF-1α levels in plasma and in liver tumour tissue samples have been reported following TACE treatment [5, 6]. A study on HCC treated by TACE [7] identified an increased proliferation of endothelial and tumour cells correlated with ischaemic necrosis. Furthermore, Increased levels of the pro-angiogenic factor vascular endothelial growth factor (VEGF) in both liver tumours and plasma samples after TACE treatment has been widely documented [5, 8, 9]. Elevated levels of VEGF in plasma post-TACE are associated with the development of metastases [10], as well as other adverse prognostic outcomes such as poor treatment response and shorter survival times [11-13]. It has been demonstrated that cells undergoing hypoxic stress in response to TACE-like ischaemia had a large increase in the quiescent population [14]. Since doxorubicin targets dividing cells by interfering with DNA replication, it is reasonable to postulate that hypoxic, quiescent cells will be more resistant to its effects. Therefore, targeted agents such as tyrosine kinase inhibitors (TKI) may be more suitable in the treatment of HCC *via* TACE, particularly those targeting the VEGF pathway.

Vandetanib is a small molecule TKI that potently inhibits VEGFR-2 and 3, as well as EGFR at a sub-micromolar concentration [2]. The anti-angiogenic effect of vandetanib has been observed in pre-clinical tumour models [15, 16]. Vandetanib also exhibits direct anti-proliferative effects on tumour cells *via* EGFR inhibition and, at higher concentrations, inhibition of FGFR and PDGFR [17, 18]. We have recently developed vandetanib-eluting radiopaque beads (VERB) for clinical use in TACE, an optimised formulation of which has been evaluated for safety and efficacy in preclinical trials [19-21]. We sought to characterise the anti-proliferative effect of vandetanib against human HCC cell lines, specifically in hypoxic conditions in order to identify any effects that inducing ischaemia *via* TACE may have on the pharmacodynamic activity of vandetanib. Our physicochemical and biological results with vandetanib and VERB suggest that this technology warrants further evaluation in clinical trials.

Results

Physico-chemical characterisation of VERB

Optical micrographs of unloaded radiopaque (RO) beads and VERB (Figure 1A) indicate that beads remain spherical and intact after loading with vandetanib, lyophilisation, gamma sterilisation and rehydration. As can be seen in Figure 1B, VERB undergo a slight decrease in average diameter as a result of the loading and lyophilisation processes, which is likely the result of a small amount of water loss upon drug loading and is reversed after extraction of the drug. To confirm imageability of VERB, beads entrapped in line phantoms to mimic vessels of varying diameters were imaged by micro-CT. Appreciable differences in radiopacity were observed in the micro CT images comparing unloaded beads and VERB (Figure 1C), reflected in an increase in average HU of almost 50%.

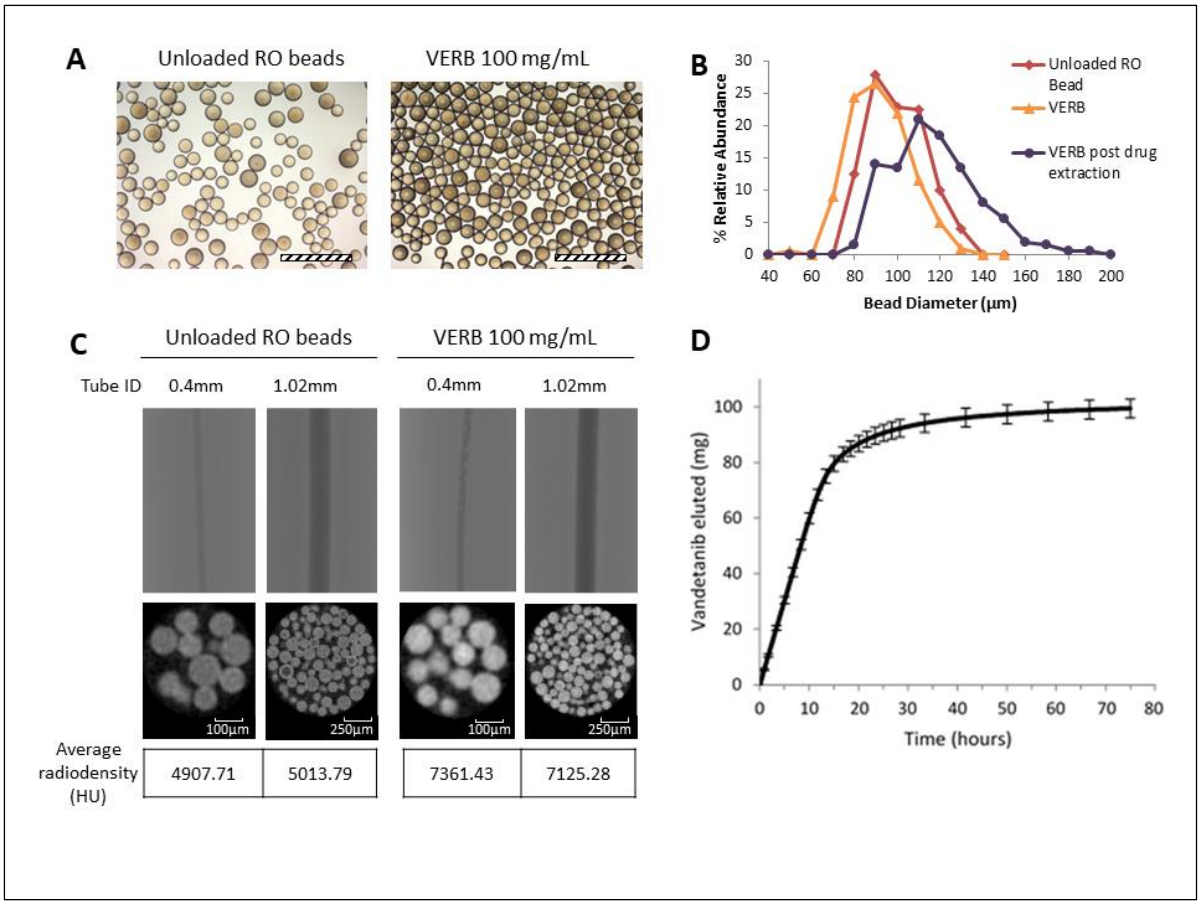

Figure 1 A) Optical micrographs of unloaded radiopaque beads (left) and beads that have been loaded with 100mg/ml vandetanib, lyophilised, gamma sterilised and rehydrated (right). Scale bars 500µm. B) Relative abundance histograms showing the distribution of beads by diameter during different stages of the drug loading process: pre-loading, loaded, sterilised and rehydrated, and post-elution beads. N=200 beads sized per sample. C) X-ray shadowgraphs of beads in line phantoms of known diameter, and µ-CT cross sections of each tube. The average radiodensity of the cross section is reported below in Hounsfield units (HU). D) Vandetanib released from 1ml of VERB in an *in vitro* open loop flow through column elution model.

Vandetanib release from VERB in an open loop *in vitro* elution model was shown to occur at a steady rate for the first 12 hours, after which the rate begins to plateau as the final 20-30 mg of drug are released (Figure 1D). 100% of the loaded dose was released by approximately 72 h, demonstrating the fully reversible binding of vandetanib to beads.

Cytotoxicity

The IC_{50} of vandetanib was determined for HCC cell lines after 72-hour exposure in normoxic or hypoxic conditions (Figure 2A). HepG2 cells were significantly more sensitive to vandetanib under hypoxic conditions than normoxia, whereas Hep3B and JHH6 showed no difference in susceptibility. Vandetanib also inhibited HUVEC proliferation in the presence of VEGF in a 24-hour period, with slightly elevated IC_{50} in hypoxic conditions.

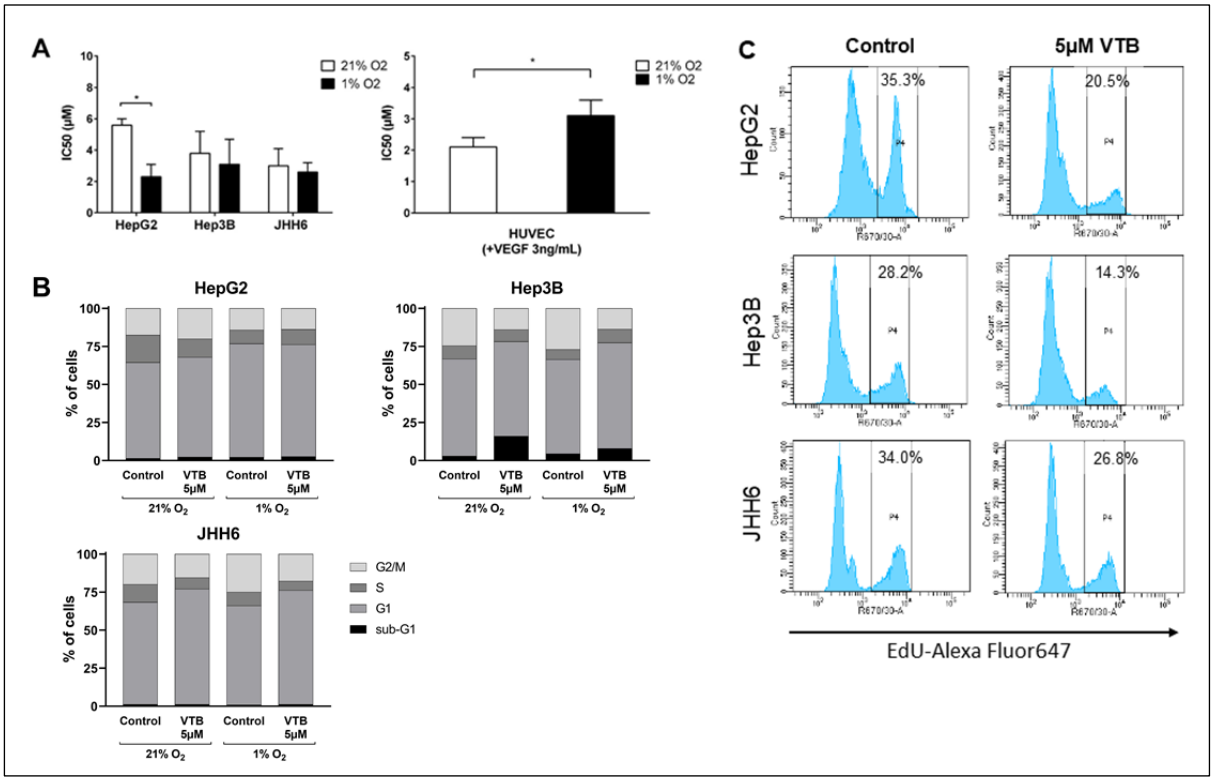

Figure 2 A) Vandetanib IC50 in normoxia (21% O2) or hypoxia (1% O2) determined using the WST-1 assay in HCC cells, 72h incubation, or HUVEC, 24h incubation in the presence of VEGF. B) Effect of 24h incubation with vandetanib (5µM) in normoxia (21%O2,) or hypoxia (1% O2) on cell cycle distribution of HCC cells. C) Flow cytometry analysis of cell proliferation by EdU uptake after 24h treatment with 5µM vandetanib in normoxia. Representative plots of 3 separate experiments.

Treatment with 5µM vandetanib for 24 hours led to mild changes in cell cycle distribution of HCC cells, which varied between cell lines (Figure 2B). An increase in the proportion of G1 phase cells for JHH6 suggested cell cycle arrest, whereas the sub-G1 fraction of Hep3B cells was increased upon vandetanib treatment indicating apoptosis. G1 arrest was confirmed by a reduction in proliferating (EdU labelled) cells when treated with vandetanib (Figure 2C). Hypoxia alone did not significantly alter cell cycle distribution in Hep3B or JHH6 cells, whereas the proliferation index (S phase %) for untreated hypoxic HepG2 cells was decreased compared with normoxic controls ($p=0.0321$) which may contribute towards their increased sensitivity to vandetanib in hypoxia.

In order to determine whether vandetanib induces apoptosis in HCC cells, flow cytometry was used to quantify Annexin V positive cells after treatment with different doses for 24 or 48 hours (Figure 3A). We observed that vandetanib-induced apoptosis was both dose and time dependent. Hep3B cells

were most susceptible, with significant apoptosis occurring after 24 and 48 hours of treatment. Accordingly, the most extensive PARP cleavage was observed in Hep3B cells (Figure 3B).

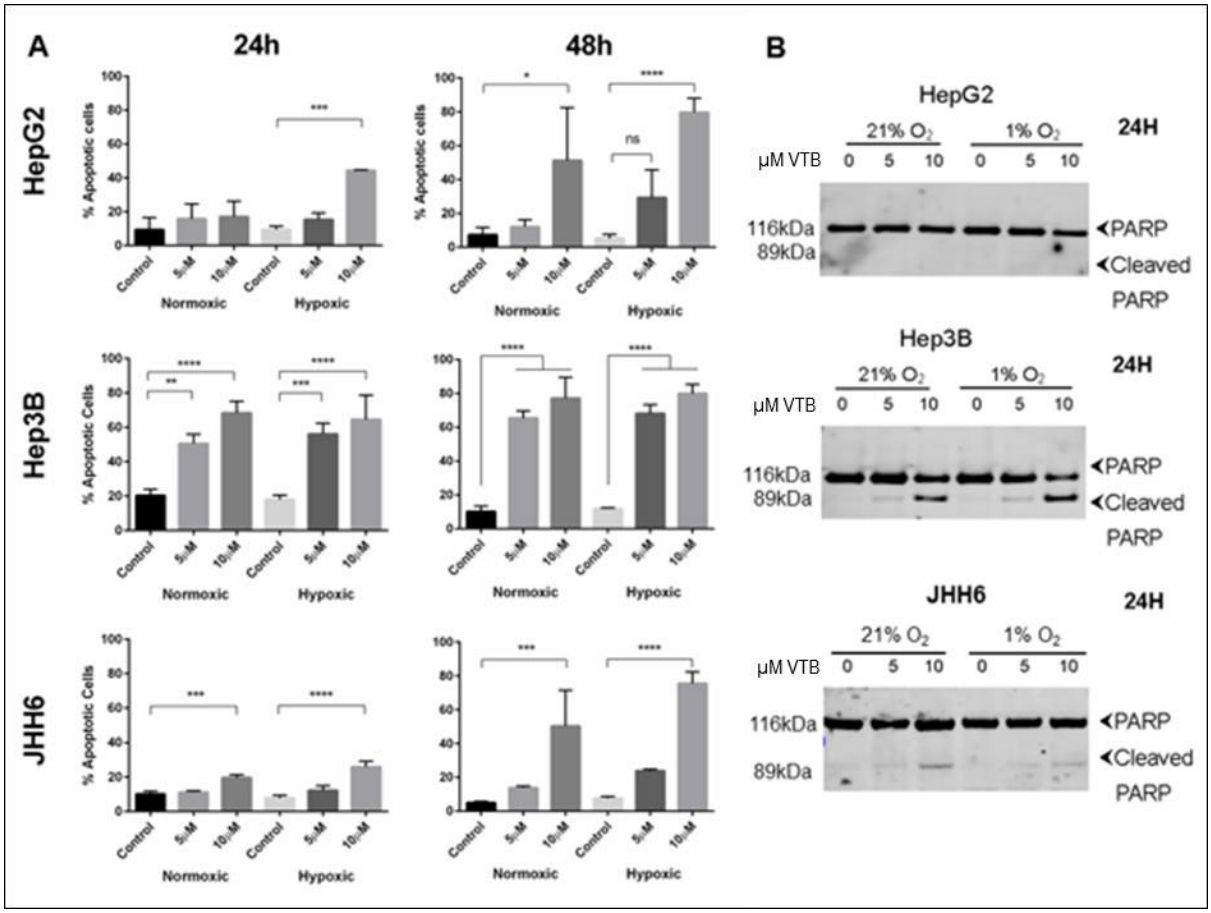

Figure 3 Vandetanib induces apoptosis in HCC cells in a dose and time dependent manner. A) Quantification of apoptotic cells by Annexin V/PI flow cytometry. B) Western blotting of full length and cleaved PARP in extracts of HCC cells treated with vandetanib for 24 hours.

Effect of vandetanib on EGFR signalling

The phosphorylation status of EGFR after vandetanib treatment of HCC cells in normoxic and hypoxic conditions was investigated using western blotting (Figure 4A). Hep3B and JHH6 cells showed strong expression of EGFR which was unaffected by vandetanib concentration and oxygen level, whereas HepG2 had low EGFR expression. Vandetanib inhibited phosphorylation of EGFR in a dose dependent manner from 1µM, and the extent of inhibition did not appear to differ between normoxic and hypoxic conditions. To determine whether EGFR inhibition affected signalling proteins further downstream, we examined the phosphorylation status of ERK1/2. Interestingly, ERK inhibition was only observed in Hep3B cells, whereas vandetanib appeared to increase ERK phosphorylation in HepG2 and JHH6 cells. Active ERK can suppress apoptosis by negatively regulating pro-apoptotic proteins such as Bim. Indeed, vandetanib treatment led to increased Bim levels, but only in Hep3B cells where ERK was successfully inhibited.

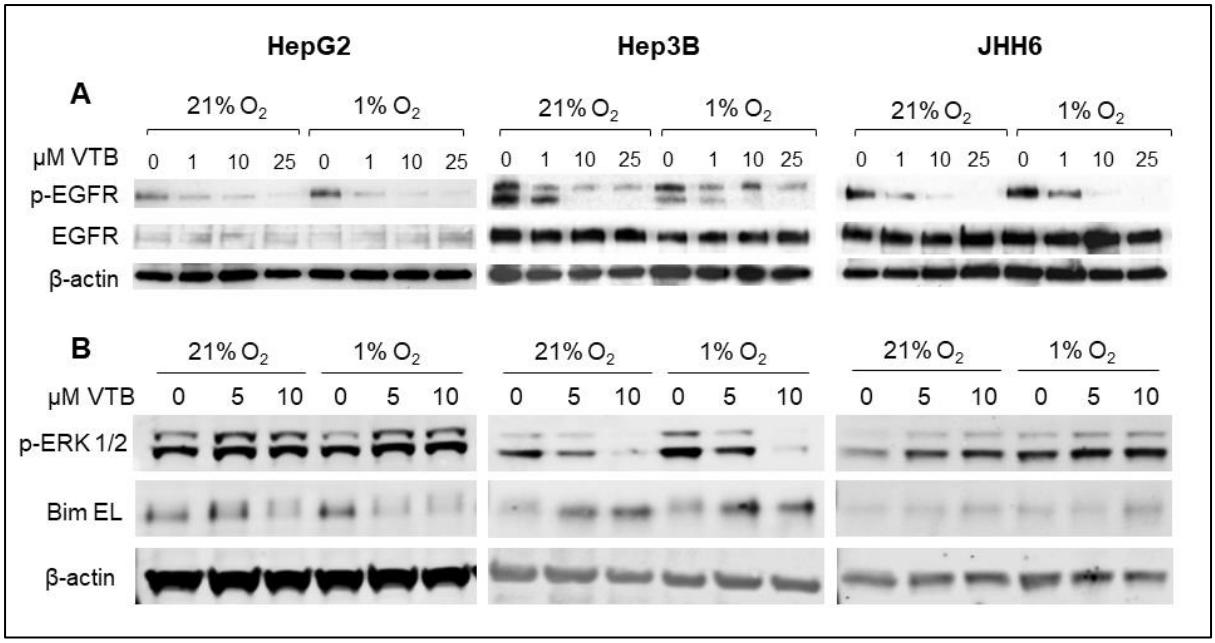

Figure 4 Western blotting of phospho-EGFR and total EGFR in cells treated with vandetanib for 4 hours followed by stimulation with EGF. B) Western blotting for phospho ERK1/2 and Bim EL in cells treated with vandetanib for 24 hours.

Effect of vandetanib on VEGF secretion

Cancer cells can stimulate angiogenesis in hypoxic conditions by secretion of VEGF. Therefore, we investigated the effect of vandetanib on VEGF secretion by HCC cells using ELISA. As expected, incubation in hypoxic conditions led to a significant increase in secreted VEGF in all HCC cell lines (Figure 5A). In normoxia, the addition of vandetanib had little effect on the levels of VEGF in the cell culture supernatant. However, in hypoxia, vandetanib caused a dose dependent reduction in VEGF levels compared to the untreated control, with doses of 25 μM bringing VEGF levels back within the range of normoxic levels.

To assess whether the reduction in VEGF secretion could be mediated by changes in HIF-1a expression, HIF-1α levels in vandetanib treated cells were assessed by ELISA (Figure 6B). As expected, HIF-1α levels were below the limit of detection in all cells cultured in normoxic conditions. In hypoxic conditions, vandetanib only affected HIF-1α levels significantly in JHH6 cells, causing a decrease at 25 μM (Figure 5B). This points to a HIF-1α independent mechanism for VEGF suppression.

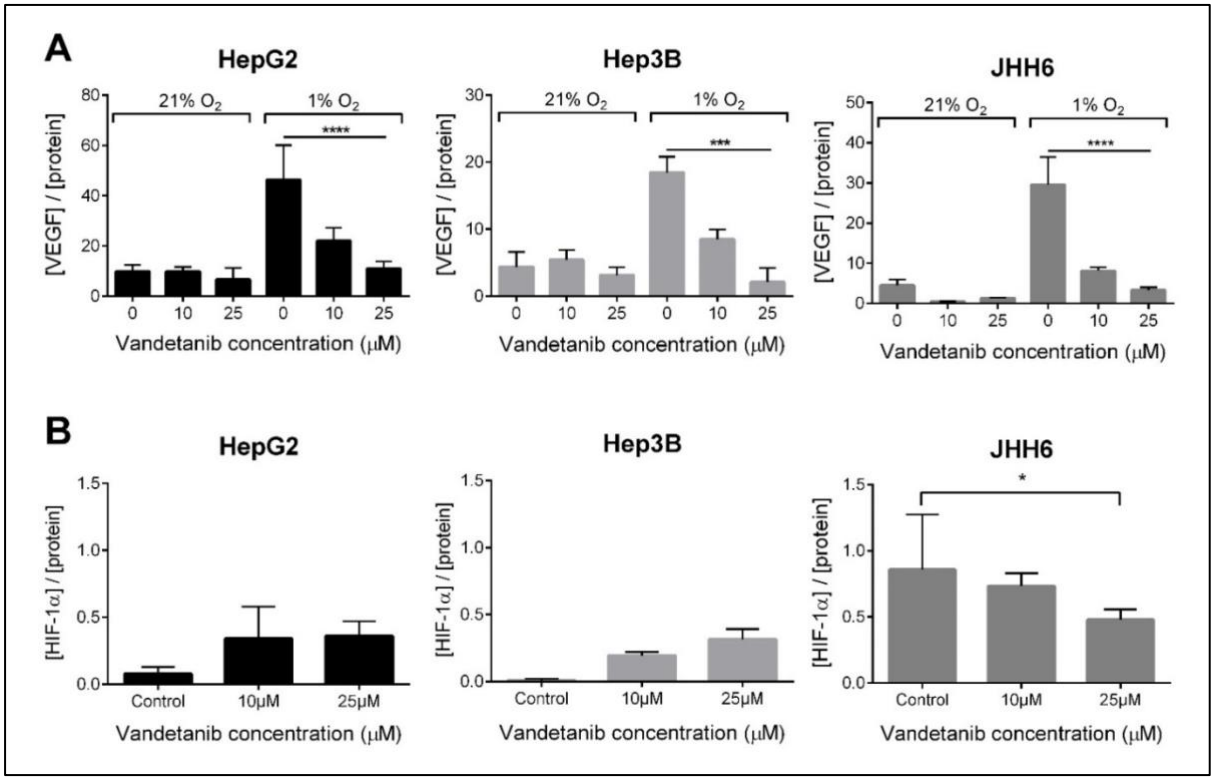

Figure 5 A) Normalised levels of VEGF in HCC cell culture supernatant after 24 hours treatment with vandetanib in normoxia (21% O2) or hypoxia (1% O2). Values were normalised to the total protein concentration in the sample. B) Normalised levels of HIF-1a in HCC cell extracts after 24 hours treatment with vandetanib in hypoxia (1% O2). Values were normalised to the total protein concentration of the sample.

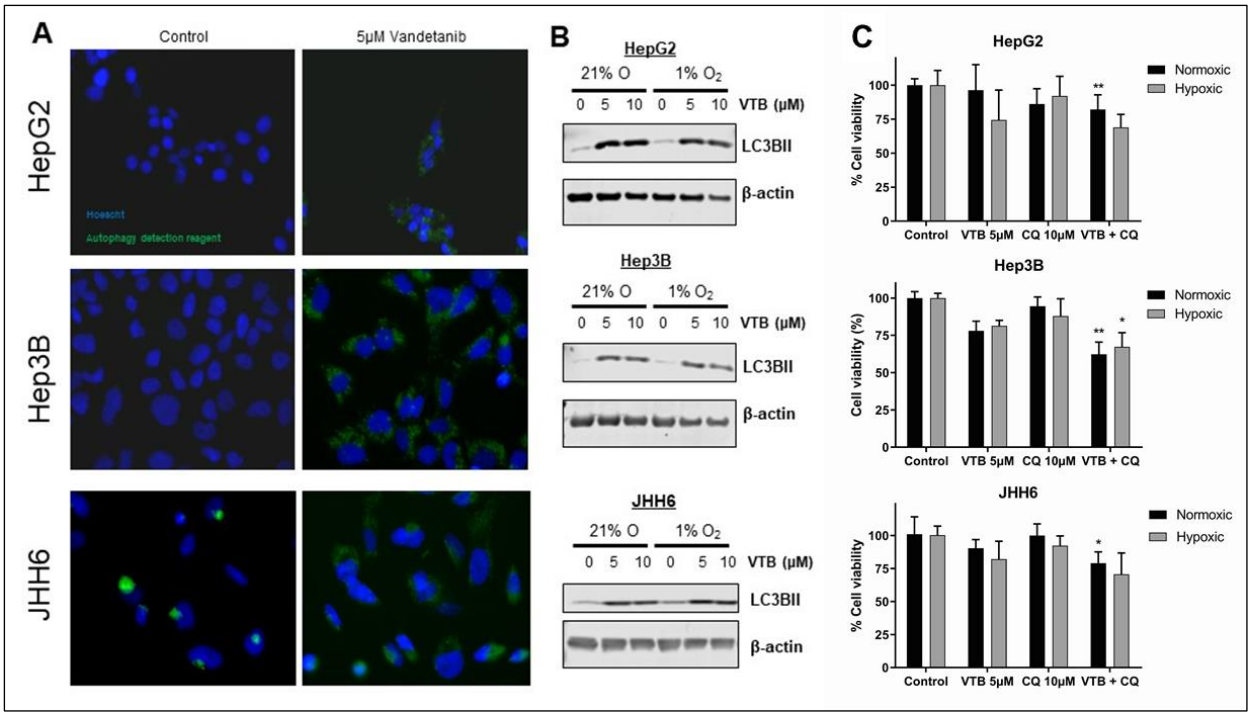

*Figure 6 Vandetanib induces autophagy in HCC cells and disrupting autophagy with chloroquine increases its efficacy. A) Fluorescent microscope images of cells treated with 5μM vandetanib for 24 hours and stained with autophagosome detection reagent (green). Nuclei counterstained with Hoescht (blue). B) Western blots for LC3BII from cells treated for 24 hours. C) Viability of cells treated with vandetanib, chloroquine or a combination of both for 24 hours, measured by resazurin assay. * p<0.05; ** p<0.01 combination vs VTB single treatment in respective oxygen condition.*

Role of autophagy

Cellular stress such as hypoxia induces autophagy, a process wherein old or damaged cellular components are digested and may be recycled as a survival mechanism [22]. We investigated the effect of vandetanib on autophagy and any impact this may have on its efficacy. Treatment with vandetanib induced autophagy in HCC cells as indicated by increased prevalence of autophagic vacuoles and increased expression of the autophagosomic protein LC3BII (Figure 6A-B). When vandetanib was combined with chloroquine, an inhibitor of autophagic flux, this led to a greater decrease in cell viability than with vandetanib treatment alone, suggesting autophagy plays a cytoprotective role (Figure 6C).

In vitro drug diffusion and effect on 3D HCC spheroids

We next sought to test the efficacy of VERB in an environment more representative of the microenvironment of an embolised tumour, using 3-D HCC spheroids. To determine the effect of bead positioning in the collagen-based 3D matrix, an experiment was conceived to directly, yet non-destructively measure the diffusion of drug species through the 3D medium. As vandetanib does not exhibit innate fluorescence in aqueous conditions, doxorubicin was used as a model drug for *in vitro* testing due to both availability and widespread use and reporting in the literature. Doxorubicin, detected by fluorescence microscopy, diffused rapidly from the bead over the course of 4 hours reaching a distance of greater than 1300 μm from the bead (Figure 7A-B). In order to approximate the concentration of vandetanib loading in a single bead, isolated beads were placed in saturated KCl:EtOH solution to extract the drug, which was quantified by HPLC using previously described methods [23]. The amount of vandetanib extracted from single beads ranged from 0.5 to 1.2 μg and had correlated positively with bead size (Figure 7C).

VERB were as effective as free vandetanib in supressing the growth of HLE spheroids over a period of 5 days, whereas bland beads had no effect on spheroid growth (Figure 7D-F). Similar effects were observed in HepG2 spheroids (Figure 7G-H).

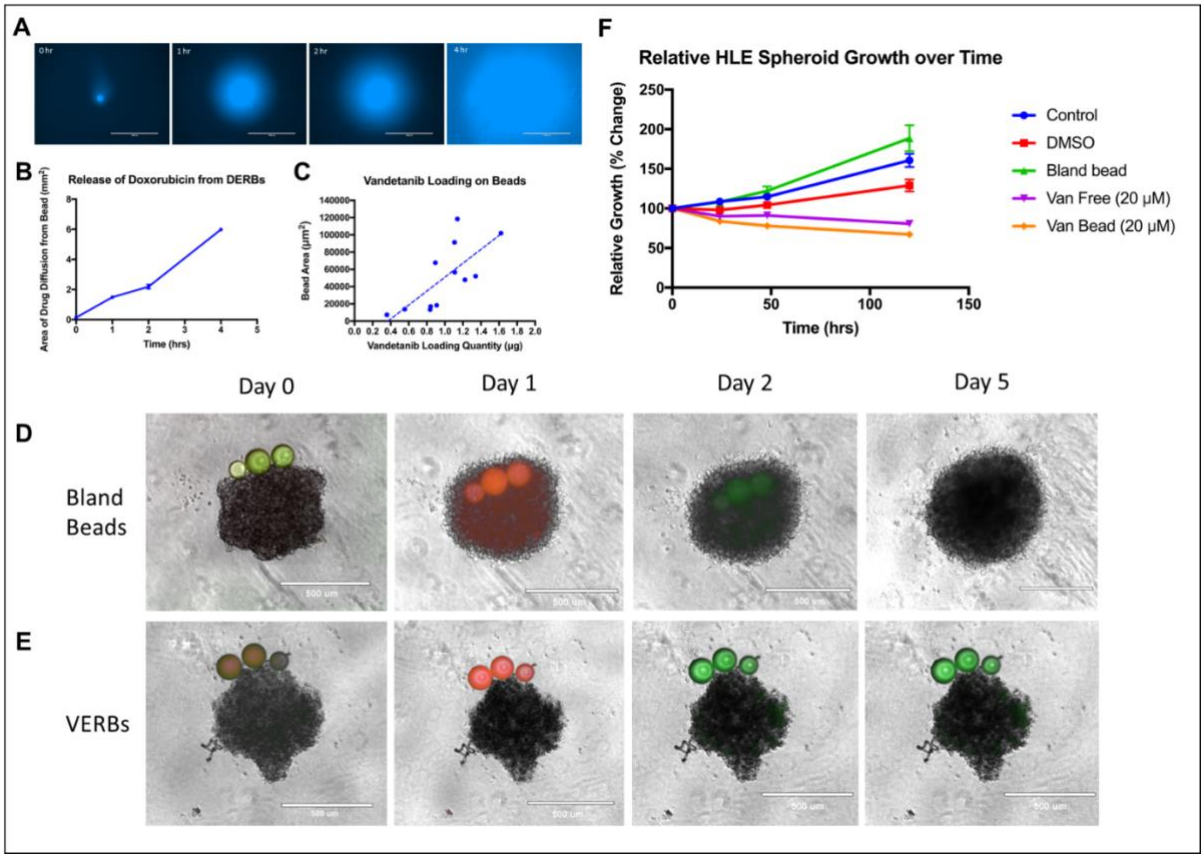

Figure 7 A&B) Doxorubicin diffusion from beads over time measured by fluorescence microscopy. C) HPLC quantification of vandetanib loading on individual VERBs as a function of planar surface area. D&E) Imaging of HLE tumour spheroids during exposure to D) bland beads or E) VERBs equivalent to 20 µM vandetanib. F) Normalised growth of HLE spheroids exposed to beads or free vandetanib. G&H) Imaging of HepG2 spheroids exposed to G) bland beads or H) VERBs.

Discussion

Chemoembolisation is the most common treatment for worldwide intermediate stage HCC, classified by the Barcelona clinic liver cancer (BCLC) staging and treatment system [24]. Although TACE has evolved over time, the chemotherapeutic agent of used for treatment has largely remained as doxorubicin. In this innovative study, we propose the use of vandetanib, a VEGFR and EGFR inhibitor whose targeted mechanism of action may prove beneficial in the locoregional treatment of HCC, as an alternative to the standard use of doxorubicin for this indication. In a phase II trial in patients with advanced HCC, oral vandetanib led to trends toward improved progression-free survival and overall survival, but results were non-significant [25]. Several studies have evaluated the combination of TACE with oral use of TKI such as sorafenib or sunitinib, with mixed results. The duration and timing of TKI administration in relation to TACE seems to be important, with trends towards improved response being observed with concurrent administration with a long duration [26-28]. Recent reports from a phase II study showed a significant improvement in time to untreatable progression (contraindication to repeated TACE sessions) with concurrent sorafenib,

showing the rationale for this treatment combination, but oral use of TKIs is associated with notable side effects, which could be reduced *via* local delivery with embolic drug-eluting beads (DEB) [29].

In our previous work, VERB was shown to be suitable for use as a DEB, with minimal changes in physicochemical properties following drug loading and sterilisation, and complete *in vitro* drug elution at a rate comparable to doxorubicin and irinotecan [30]. *In vivo*, therapeutic levels of vandetanib were found in swine livers treated with VERB-TACE 30 days after embolization [20], which may be a function of the long half-life of vandetanib (19 days in humans [31]), but also indicates that *in vivo* drug release likely takes place at a slower rate in tissue. This is due to sequestration of beads in blocked blood vessels with complete stasis of blood flow in some cases. We have recently reported a more thorough investigation into mimicking in vivo conditions for in vitro release studies elsewhere [23]. Loading of vandetanib into RO beads has previously been shown to induce a dose dependent increase in radiopacity, which is likely due to the presence of radiodense bromine atoms from the drug that contribute to the absorption of the x-rays [19]. Unloaded RO bead image intensity under CT is known not to decrease over a period of at least 90 days in vivo [32]. Therefore, if the added radiopacity bestowed by vandetanib is reversible upon drug release, this characteristic has interesting implications for a potential surrogate marker of vandetanib release *in vivo*. However, further studies would be required to validate this approach.

Despite its proven role in cancer drug resistance, there is little published research on the effect of hypoxia on the efficacy of vandetanib. We showed that hypoxia did not cause resistance to vandetanib in a panel of 3 HCC cell lines in terms of proliferation and apoptosis rates, and even augmented the response to vandetanib in HepG2 cells. However, this did not appear to be related to differences in EGFR expression or inhibition in hypoxia. Fujita and colleagues demonstrated that hypoxia (1% O_2) inhibited proliferation of HepG2 cells by causing G1 phase cell cycle arrest, which could provoke resistance to DNA replication inhibitors such as doxorubicin [33]. This is not the case for vandetanib. Instead, hypoxia may lower the threshold for apoptosis induced by vandetanib in HepG2 cells, which are the only cell line in our panel to express wild type p53, a key regulator of cell cycle arrest and apoptosis in response to cellular stress [34].

We hypothesised that the induction of apoptosis by vandetanib was related to inhibition of EGFR phosphorylation, which was consistently observed among the cell lines tested. Bim is a pro-apoptotic protein that has previously shown to be required for TKI-induced cell death [35], and is in turn negatively regulated by ERK, a key downstream effector in the EGFR pathway. When we studied phospho-ERK and Bim expression, there were marked differences among the cell lines: ERK inhibition and Bim upregulation was observed, but only in Hep3B cells. Despite this, vandetanib still induced apoptosis in the other cell lines, albeit to a lesser extent, suggesting an alternative pathway independent of Bim.

We demonstrated that vandetanib can induce both direct and indirect effects on angiogenesis, by inhibiting HUVEC proliferation and reducing the expression of VEGF in HCC cells, respectively. The decrease in VEGF levels was particularly evident in hypoxic conditions, but changes in HIF-1α expression were not observed. Therefore, the mechanism may be due to EGFR inhibition, which in turn suppresses the Sp1 transcription factor binding to VEGF promoter *via* Akt inhibition as has been demonstrated with EGFR inhibitor gefitinib [36].

Several studies have identified autophagy as a mechanism of resistance to TKI [37, 38]. Autophagy is activated in response to cellular stresses such as nutrient deprivation, and hypoxia, which is relevant to our study. We too found that vandetanib treatment induced autophagy in HCC cells, and blocking it with chloroquine modestly augmented the efficacy of vandetanib, an effect that may be more pronounced with longer incubation times given the time dependent action of vandetanib. The efficacy of combining autophagy inhibition and TKI has been shown to translate to *in vivo* conditions [39]. There are currently two ongoing phase I-II clinical trials investigating the combination of hydroxychloroquine and TACE or hydroxychloroquine and sorafenib in the treatment of HCC, which will provide a preliminary insight into the efficacy of this approach [40, 41]; alternative inhibitors of the autophagy pathway with greater potency and selectivity are also under evaluation [42].

Finally, we demonstrated the efficacy of VERB in 3D tumour spheroids of HCC. Implantation of only 3 microspheres were found to have an equivalent antiproliferative effect to 20 µM free drug over the same time period of treatment. Importantly, this result indicated that the elution of vandetanib was rapid and equal in these conditions. It also suggested the 3-D environment, with its unperfused, partially hypoxic cell mass, may recreate the embolised tumour microenvironment and, in line with other 2-D results, suggests vandetanib will have anticancer effects in embolised tumours. Although the vandetanib concentration required to completely suppress spheroid growth was higher than the average IC_{50} determined in 2-D cell culture, it remains a concentration that is achievable with local drug delivery from DEB [43-45] Indeed, initial tissue concentrations of drugs surrounding implanted DEB have been reported to be as high as 30-40µM [45].

We have demonstrated the efficacy of vandetanib eluting radiopaque beads in cell culture models of HCC and demonstrated new mechanisms of action of vandetanib following local embolic delivery. Based on these data, we have planned a first-in-human clinical study in patients with cancer and results are anticipated in early 2020 [46].

Materials and Methods

Preparation and physical characterisation of vandetanib-eluting beads

Vandetanib-eluting radiopaque beads (VERB) were prepared at a loading dose of 100mg vandetanib per mL of beads as previously described [20]. Briefly, radiopaque (RO) beads (70-150µm diameter range) were loaded with vandetanib by immersion in the drug solution with shaking for 2 hours. Loaded beads were frozen, lyophilised and sterilised by gamma irradiation (25Gy). Prior to experimental use, purified water was added to dry beads which were gently swirled and left for 30 minutes to rehydrate. Bead size characterisation was performed by examining beads under an optical microscope and recording the diameter of 200 beads per sample using Stream software (Olympus). To assess radiopacity, line phantoms to mimic embolised blood vessels were prepared by filling tubes of known internal diameter (0.4mm or 1.02mm) with RO beads or VERB prior to setting in place in a nunc tube filled with agarose solution. The line phantoms were imaged by micro-CT at Reading Scientific Services ltd. using a Bruker SkyScan 1172 micro-CTscanner (Kontich, Belgium). Each bead phantom was imaged at 64 kVp, 155 µA with an aluminium filter (500µm). The samples were then reconstructed using NRecon and calibrated against a volume of interest of air and purified water to yield average Hounsfield Units (HU) of each sample.

In vitro drug release testing

To assess the release rate of vandetanib from VERB under representative conditions, an in-house, open loop flow through elution model was used as previously described [47]. Rehydrated beads were sandwiched between two filter membranes in an elution cell, which was submerged in a water bath at 37°C. Fresh PBS was continuously pumped through the cell at a flow rate of 1.7mL/min. Vandetanib levels in the PBS leaving the cell over time were quantified *via* an automated UV detector (330nm).

In vitro drug diffusion

Lone bead samples of Doxorubicin-eluting embolic beads were isolated under magnification and injected into amorphous collagen matrix in a 96 well plate kept on ice before being transferred to an EVOS FL fluorescence microscope (Thermo-Fisher, USA) for fluorescent detection of the doxorubicin analyte. Following the initial measurement, the sample was placed in the incubator at 37°C to both allow the amorphous matrix to set and to replicate the procedure used for other *in vitro* studies. The well plate was removed from the incubator at regular one hour intervals to repeat the fluorescent imaging before being replaced in the incubator.

Bead loading quantification

Single bead samples were extracted under magnification from a 1 mL vial containing Vandetanib-loaded TACE beads with a 2 µL micropipette, photographed at 10x magnification with an EVOS FL microscope (Thermo-Fisher, USA) to determine the radius of each bead, and placed in 25 µL 50:50 KCl:EtOH (pH 14) (Prepared with reagents from Sigma-Aldrich, USA) drug extraction solution according to methods described previously [48]. After 24 hours of extraction, the beads were removed under magnification and the remaining solution was analysed with HPLC according to previously described methods for quantification of vandetanib dose [19].

Cell lines and culture

HepG2 cells were purchased from European Collection of Authenticated Cell Cultures (ECACC 85011430) and maintained in Minimum Essential Medium (Gibco) supplemented with 10% fetal bovine serum (FBS) and 1% non-essential amino acids (NEAA, Gibco). Hep3B cells were a gift from Dr. Armand de Gramont at the Department of Oncology, CHUV, Switzerland and were maintained in RPMI 1640 (Gibco) with 10% FBS. JHH6 cells were purchased from the Japanese Collection of Research Bioresources Cell Bank (JCRB1030, original depositor Dr. Seishi Nagamori) and cultured in RPMI 1640 with 10% FBS.

Pooled donor HUVECs pre-screened for expression of angiogenesis markers (Axl, eNOS, Tie-2, VEGFR-2) were purchased from Lonza (Cat. no. C2519AS) and were cultured in Endothelial Growth Medium (EGM-2, Lonza) consisting of Endothelial Basal Medium supplemented with EGM-2 Bullet Kit containing FBS (final concentration 2%) and endothelial growth supplements.

Cells for spheroid culture were grown as above with HLE cells grown in Dulbecco's Modified Eagle Medium (DMEM) supplemented with 10% FBS and 1% NEAA. Confluent cells were trypsinised and 5000 cells per well were plated on ultra-low attachment U-bottomed 96-well plates and centrifuged under 200 G forces for 3 minutes before being replaced in the incubator for 5 days at 37°C. After 5

days, the media was removed from the wells and replaced with a 3-D matrix comprised of Matrigel (Corning) and DMEM at which point beads or free drug were added to the well.

Hypoxic (1% O_2) cell incubation was performed in an invivO2 hypoxia chamber (Baker Ruskinn, UK).

Preparation of drug solutions for cell culture experiments

10mM vandetanib (Astra Zeneca, UK) stock solution was prepared in DMSO. The stock solution was sterile filtered using a 0.2 µm pore sterile syringe filter (Corning) and subsequent dilutions of the stock solutions in cell culture medium were performed in sterile conditions prior to use. The concentration of DMSO was kept consistent across all experimental conditions including controls.

HCC Cell viability assays

HCC cells were seeded into 96 well plates (Costar) and allowed to equilibrate in normoxic conditions for 24 hours. At this point, media was aspirated from the cells and replaced with media containing vandetanib of concentrations ranging from 0 – 50 µM. After addition of drug, plates were placed in either the normoxic (21% O_2) or hypoxic (1% O_2) incubator for 72 hours. At the end of the incubation period, 20 µL of WST-1 reagent (Takara) was added to each well and the plate was placed back into the respective incubator for 30 minutes. The absorbance was read on a multi-well plate reader at 440nm (ref 630nm).

HUVEC proliferation assay

HUVECs were seeded in supplemented EGM-2 (2% FBS) at a density of 2500 cells per well in a 96 well plate and allowed to equilibrate for 24 hours in normoxic conditions. The media was removed and replaced with EBM-2 (basal medium) containing 2% FBS and 3 ng/mL VEGF (Peprotech) with vandetanib ranging from 0-20 µM and incubated for 24 hours in either normoxic or hypoxic conditions. 20 µL of WST-1 reagent was added to each well and incubated for 1 hour. Absorbance was read in a multi-well plate reader as before.

Cell cycle analysis and EdU incorporation assay

Cells were seeded in 6cm plates and allowed to equilibrate overnight in normoxic conditions. Cells were then treated with DMSO or 5µM vandetanib for 24 hours in normoxic or hypoxic conditions. Cells were then fixed in ethanol, stained with propidium iodide and analysed by flow cytometry (BD Fortessa X20). Output data were analysed with FlowJo® flow cytometry software in order to determine cell cycle distribution.

Cells treated with 5µM vandetanib for 24 hours in normoxic or hypoxic conditions were incubated with 10mM EdU for 30 minutes at the end of drug treatment and analysed for EdU incorporation using the Click-iT™ EdU Alexa Fluor™ 647 Flow Cytometry Assay Kit (Invitrogen) according to the manufacturer's instructions.

Annexin V/PI flow cytometry

HCC cells were treated with vandetanib for 24 or 48 hours in normoxic or hypoxic conditions. Apoptotic cells were labelled with the Dead Cell Apoptosis Kit with Annexin V FITC and PI (Invitrogen) according to manufacturer's instructions and analysed by flow cytometry. Annexin V positive cells were classified as apoptotic.

Western blotting

HCC cells were lysed in RIPA buffer and the protein concentration determined by Bradford assay (Sigma-Aldrich). Samples were separated in precast 4-12% bis-tris gels (Novex) and transferred to a PVDF membrane. Membranes were blocked for 1 hour in blocking buffer (Licor) and probed with primary antibodies against phospho-EGFR (Ab32086, 1:3000), EGFR (Ab32077, 1:6000), phospho-ERK1/2 (Ab76299, 1:1000), PARP (BD Pharmingen 51-6639GR, 1:1000), BIM (Cell signalling #2933, 1:1000), LC3BII (Cell signalling #3868, 1:2000), or β-actin (Ab8226, 1:10000) diluted in blocking buffer, overnight at 4 °C, followed by fluorophore conjugated secondary antibody 1:10000 in blocking buffer for 1 hour at room temperature. The bands were visualised using the Licor Odyssey CLX near-infrared fluorescence imaging system.

Measurement of VEGF in cell culture supernatants

HCC cells were seeded in 24 well plates and allowed to equilibrate for 24 hours or until approximately 70% confluent. After washing cells in PBS, the culture medium was replaced with serum-free medium containing 0, 10 or 25 μM vandetanib, and cells were incubated in normoxia or hypoxia for 24 hours. The conditioned culture medium was then harvested and stored at -20 °C. VEGF levels in the culture medium were quantified by a commercial VEGF ELISA kit (ab100662, Abcam) and normalised to the protein content of each sample as determined by Bradford assay (Sigma Aldrich).

Measurement of HIF-1α levels

Levels of HIF-1α were measured using a HIF-1α ELISA kit (ab171577, Abcam) according to manufacturer's instructions. HCC cells were seeded in 6 well plates and incubated until 80% confluent. Culture medium was replaced with serum-free medium containing 0, 10 or 25 μM vandetanib or doxorubicin, and cells were incubated in normoxia or hypoxia for 24 hours. To harvest cell extracts, the cells were washed in cold PBS and lysed in lysis buffer supplied with the ELISA kit. Lysates were stored at -80 °C until use. HIF-1α levels in the cell extracts were quantified by ELISA and normalised to protein content of each sample as determined by Bradford assay (Sigma Aldrich).

Detection of autophagy

Autophagosomes were detected in treated cells using an autophagy detection kit (ab139484, Abcam) according to manufacturer's instructions. Cells were treated with vandetanib or chloroquine (10μM) for 24 hours and stained with the 488nm-excitable autophagosome detection reagent and Hoescht. Cells were visualised using fluorescence microscopy (EVOS) with FITC and DAPI filters.

Author Contributions

A.H. conducted the experiments for figures 1-6 and wrote the main manuscript text. S.Z. conducted the 3D spheroid experiments, prepared figure 7 and participated in drafting and revision of the manuscript. A.W. and R.C. conducted and analysed data from the cell cycle experiments. W.M.M., G.P., A.W.L., R.A.S. and A.L. jointly supervised the project, participated in discussion of data and its analysis and contributed to the manuscript preparation.

Acknowledgments

This work was partially funded by an industrial fellowship from the Royal Commission for the Exhibition of 1851 and by the NIHR University College London Hospitals Biomedical Research Centre and CRUK UCL Experimental Cancer Medicines Centre.

References

1. Hong, K., et al., *New intra-arterial drug delivery system for the treatment of liver cancer: preclinical assessment in a rabbit model of liver cancer.* Clin Cancer Res, 2006. **12**(8): p. 2563-7.
2. Wedge, S.R., et al., *ZD6474 Inhibits Vascular Endothelial Growth Factor Signaling, Angiogenesis, and Tumor Growth following Oral Administration.* Cancer research, 2002. **62**(16): p. 4645-4655.
3. Li, Q., et al., *Cytotoxic activity of anticancer drugs on hepatocellular carcinoma cells in hypoxic-hyponutritional culture.* Int Surg, 2014. **99**(6): p. 745-52.
4. Rohwer, N. and T. Cramer, *Hypoxia-mediated drug resistance: Novel insights on the functional interaction of HIFs and cell death pathways.* Drug Resistance Updates, 2011. **14**(3): p. 191-201.
5. Liang, B., et al., *Correlation of Hypoxia-Inducible Factor 1[alpha] with Angiogenesis in Liver Tumors After Transcatheter Arterial Embolization in an Animal Model.* Cardiovascular and Interventional Radiology, 2010. **33**(4): p. 806-12.
6. Jia, Z.-z., G.-m. Jiang, and Y.-l. Feng, *Serum HIF-1α and VEGF Levels Pre- and Post-TACE in Patients with Primary Liver Cancer.* Chinese Medical Sciences Journal, 2011. **26**(3): p. 158-162.
7. Kim, Y.B., Y.N. Park, and C. Park, *Increased proliferation activities of vascular endothelial cells and tumour cells in residual hepatocellular carcinoma following transcatheter arterial embolization.* Histopathology, 2001. **38**(2): p. 160-166.
8. Li, X., et al., *Expression of plasma vascular endothelial growth factor in patients with hepatocellular carcinoma and effect of transcatheter arterial chemoembolization therapy on plasma vascular endothelial growth factor level.* World Journal of Gastroenterology, 2004. **10**(19): p. 2878-2882.
9. Wang, B., XU, H., GAO, Z. Q., NING, H. F., SUN, Y. Q. & CAO, G. W., *Increased expression of vascular endothelial growth factor in hepatocellular carcinoma after transcatheter arterial chemoembolization.* Acta Radiologica, 2008. **49**(5): p. 523-529.
10. Xiong, Z.P., et al., *Association between vascular endothelial growth factor and metastasis after transcatheter arterial chemoembolization in patients with hepatocellular carcinoma.* Hepatobiliary Pancreat Dis Int, 2004. **3**(3): p. 386-90.
11. Poon, R.T., Lau, C., Yu, W., Fan, S., Wong, J., *High serum levels of vascular endothelial growth factor predict poor response to transarterial chemoembolization in hepatocellular carcinoma: A prospective study.* Oncology Reports, 2004. **11**(5): p. 1077-1084.
12. Sergio, A., et al., *Transcatheter arterial chemoembolization (TACE) in hepatocellular carcinoma (HCC): the role of angiogenesis and invasiveness.* Am J Gastroenterol, 2008. **103**(4): p. 914-21.
13. Shim, J.H., et al., *Association between increment of serum VEGF level and prognosis after transcatheter arterial chemoembolization in hepatocellular carcinoma patients.* Cancer Science, 2008. **99**(10): p. 2037-2044.
14. Gade, T.P., et al., *Targeting the metabolic stress response in hepatocellular carcinoma to potentiate TACE-induced ischemia.* Journal of Vascular and Interventional Radiology, 2015. **26**(2): p. S17.
15. Bradley, D.P., et al., *Effects of AZD2171 and vandetanib (ZD6474, Zactima) on haemodynamic variables in an SW620 human colon tumour model: an investigation using dynamic contrast-enhanced MRI and the rapid clearance blood pool contrast agent, P792 (gadomelitol).* NMR in Biomedicine, 2008. **21**(1): p. 42-52.
16. Tai, J.H., et al., *Assessment of Acute Antivascular Effects of Vandetanib with High-Resolution Dynamic Contrast-Enhanced Computed Tomographic Imaging in a Human Colon Tumor Xenograft Model in the Nude Rat.* Neoplasia, 2010. **12**(9): p. 697-707.
17. Inoue, K., et al., *Vandetanib, an Inhibitor of VEGF Receptor-2 and EGF Receptor, Suppresses Tumor Development and Improves Prognosis of Liver Cancer in Mice.* Clinical Cancer Research, 2012. **18**(14): p. 3924-3933.

18. Liu, S., et al., *Use of protein array technology to investigate receptor tyrosine kinases activated in hepatocellular carcinoma.* Experimental and Therapeutic Medicine, 2011. **2**(3): p. 399-403.
19. Hagan, A., et al., *Preparation and characterisation of vandetanib-eluting radiopaque beads for locoregional treatment of hepatic malignancies.* European Journal of Pharmaceutical Sciences, 2017. **101**: p. 22-30.
20. Denys, A., et al., *Vandetanib-eluting Radiopaque Beads: In vivo Pharmacokinetics, Safety and Toxicity Evaluation following Swine Liver Embolization.* Theranostics, 2017. **7**(8): p. 2164-2176.
21. Duran, R., et al., *Vandetanib-eluting Radiopaque Beads: Pharmacokinetics, Safety, and Efficacy in a Rabbit Model of Liver Cancer.* Radiology, 2019: p. 190305.
22. Tan, Q., et al., *Role of Autophagy as a Survival Mechanism for Hypoxic Cells in Tumors.* Neoplasia (New York, N.Y.), 2016. **18**(6): p. 347-355.
23. Hagan, A., et al., *Predicting pharmacokinetic behaviour of drug release from drug-eluting embolization beads using in vitro elution methods.* European Journal of Pharmaceutical Sciences, 2019. **136**: p. 104943.
24. Forner, A., M. Reig, and J. Bruix, *Hepatocellular carcinoma.* The Lancet, 2018. **391**.
25. Hsu, C., et al., *Vandetanib in patients with inoperable hepatocellular carcinoma: a phase II, randomized, double-blind, placebo-controlled study.* J Hepatol, 2012. **56**(5): p. 1097-103.
26. Lencioni, R., et al., *Sorafenib or placebo plus TACE with doxorubicin-eluting beads for intermediate stage HCC: The SPACE trial.* J Hepatol, 2016. **64**(5): p. 1090-8.
27. Kudo, M., et al., *Phase III study of sorafenib after transarterial chemoembolisation in Japanese and Korean patients with unresectable hepatocellular carcinoma.* European Journal of Cancer. **47**(14): p. 2117-2127.
28. Geschwind, J.F., et al., *TACE Treatment in Patients with Sorafenib-treated Unresectable Hepatocellular Carcinoma in Clinical Practice: Final Analysis of GIDEON.* Radiology, 2016. **279**(2): p. 630-40.
29. Kudo, M., et al., *Randomized, open label, multicenter, phase II trial comparing transarterial chemoembolization (TACE) plus sorafenib with TACE alone in patients with hepatocellular carcinoma (HCC): TACTICS trial.* Journal of Clinical Oncology, 2018. **36**(4_suppl): p. 206-206.
30. Ashrafi, K., et al., *Characterization of a novel intrinsically radiopaque Drug-eluting Bead for image-guided therapy: DC Bead LUMI™.* Journal of Controlled Release, 2017. **250**: p. 36-47.
31. FDA, *Clinical Pharmacology Review: Vandetanib*. 2010.
32. Sharma, K.V., et al., *Long-term biocompatibility, imaging appearance and tissue effects associated with delivery of a novel radiopaque embolization bead for image-guided therapy.* Biomaterials, 2016. **103**: p. 293-304.
33. Fujita, H., et al., *Metformin attenuates hypoxia-induced resistance to cisplatin in the HepG2 cell line.* Oncology Letters, 2019. **17**: p. 2431-2440.
34. Humpton, T.J. and K.H. Vousden, *Regulation of Cellular Metabolism and Hypoxia by p53.* Cold Spring Harbor perspectives in medicine, 2016. **6**(7): p. a026146.
35. Costa, D.B., et al., *BIM Mediates EGFR Tyrosine Kinase Inhibitor-Induced Apoptosis in Lung Cancers with Oncogenic EGFR Mutations.* PLOS Medicine, 2007. **4**(10): p. e315.
36. Pore, N., et al., *EGFR Tyrosine Kinase Inhibitors Decrease VEGF Expression by Both Hypoxia-Inducible Factor (HIF)-1–Independent and HIF-1–Dependent Mechanisms.* Cancer research, 2006. **66**(6): p. 3197-3204.
37. Han, W., et al., *EGFR Tyrosine Kinase Inhibitors Activate Autophagy as a Cytoprotective Response in Human Lung Cancer Cells.* PLOS ONE, 2011. **6**(6): p. e18691.
38. Shen, J., et al., *Autophagy inhibition induces enhanced proapoptotic effects of ZD6474 in glioblastoma.* Br J Cancer, 2013. **109**(1): p. 164-71.
39. Shimizu, S., et al., *Inhibition of autophagy potentiates the antitumor effect of the multikinase inhibitor sorafenib in hepatocellular carcinoma.* International Journal of Cancer, 2012. **131**(3): p. 548-557.

40. Clinicaltrials.gov. *Identifier: NCT03037437, Sorafenib Induced Autophagy Using Hydroxychloroquine in Hepatocellular Cancer.* 2017 [cited 2019 15/09/19]; Available from: https://clinicaltrials.gov/ct2/show/NCT03037437.
41. Clinicaltrials.gov. *Identifier: NCT02013778, Phase1-2 Trial HCQ Plus TACE in Unresectable HCC.* 2013 [cited 2019 15/09/19]; Available from: https://clinicaltrials.gov/ct2/show/NCT02013778.
42. Wang, C., Q. Hu, and H.M. Shen, *Pharmacological inhibitors of autophagy as novel cancer therapeutic agents.* Pharmacol Res, 2016. **105**: p. 164-75.
43. Namur, J., et al., *Embolization of hepatocellular carcinoma with drug-eluting beads: doxorubicin tissue concentration and distribution in patient liver explants.* J Hepatol, 2011. **55**(6): p. 1332-8.
44. Namur, J., et al., *Drug-eluting beads for liver embolization: concentration of doxorubicin in tissue and in beads in a pig model.* J Vasc Interv Radiol, 2010. **21**(2): p. 259-67.
45. Dreher, M.R., et al., *Radiopaque Drug-Eluting Beads for Transcatheter Embolotherapy: Experimental Study of Drug Penetration and Coverage in Swine.* Journal of Vascular and Interventional Radiology, 2012. **23**(2): p. 257-264.e4.
46. Beaton, L., et al., *VEROnA Protocol: A Pilot, Open-Label, Single-Arm, Phase 0, Window-of-Opportunity Study of Vandetanib-Eluting Radiopaque Embolic Beads (BTG-002814) in Patients With Resectable Liver Malignancies.* JMIR Res Protoc, 2019. **8**(10): p. e13696.
47. Swaine, T., et al., *Evaluation of ion exchange processes in drug-eluting embolization beads by use of an improved flow-through elution method.* European Journal of Pharmaceutical Sciences, 2016. **93**: p. 351-359.
48. Caine, M., et al., *Review of the Development of Methods for Characterization of Microspheres for Use in Embolotherapy: Translating Bench to Cathlab.* Adv Healthc Mater, 2017. **6**(9).